Figures

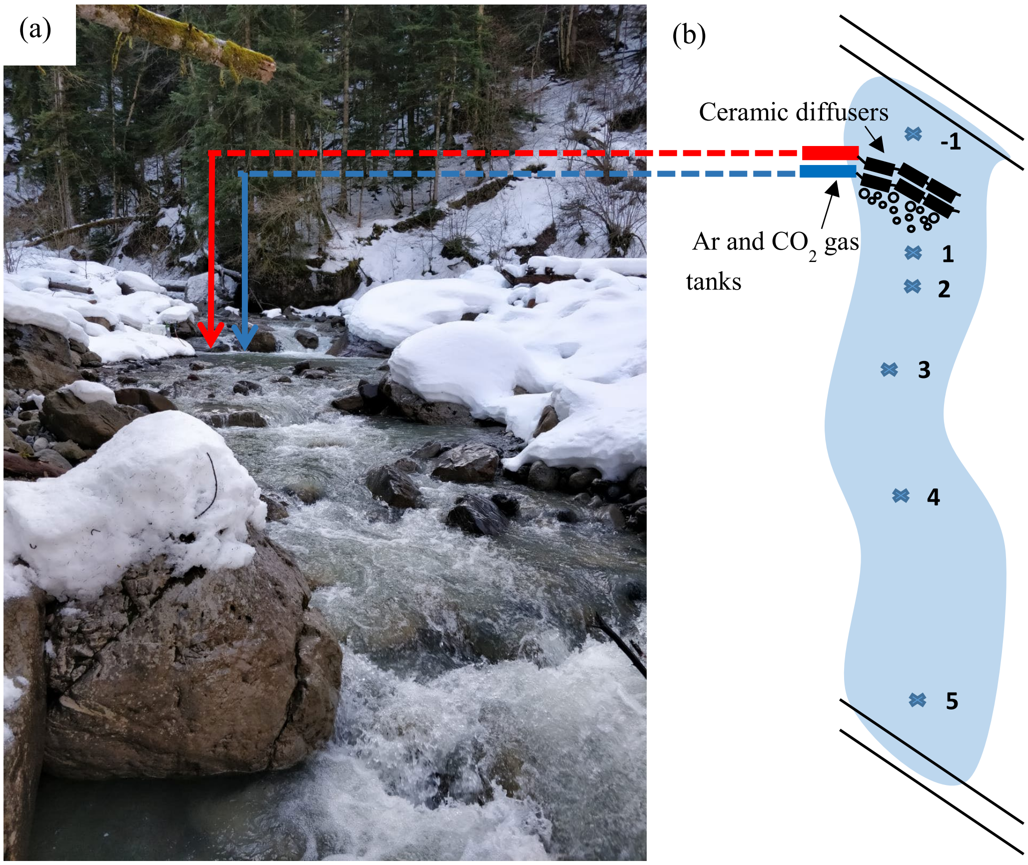

Figure 1. a) Photo of one of the experiment streams (Veveyse) taken on March 12th 2019 and **b**) Schematic of the experimental set up showing the stations -1 through 5. The ceramic diffusers for this particular release were placed at the location designated by the red and blue arrows in Figure 1. a).

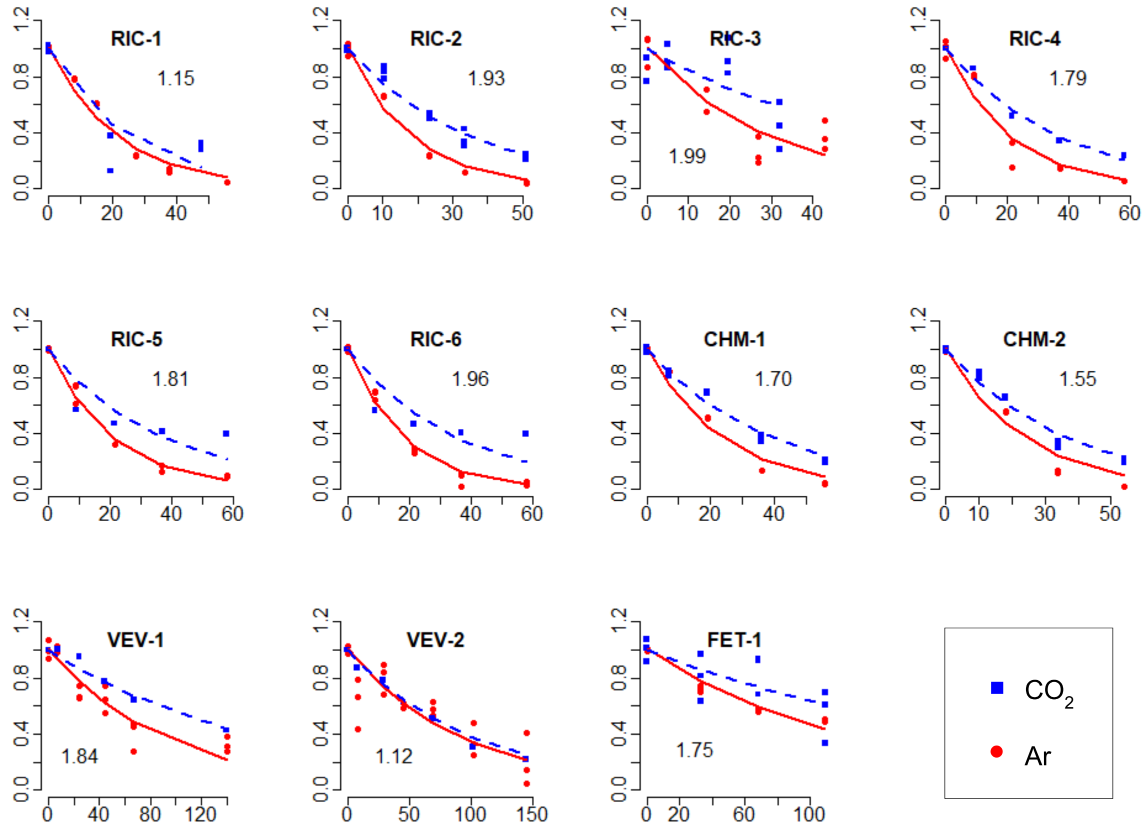

Figure 2. Exponential decline of normalized Ar (red) and CO_2 (blue), sampled at stations along the reach at each study site. Lines are exponential models fitted to the points of normalized gas concentration. Values for *a* estimated at each site are shown on each plot and ranged from 1.12 to 1.96.

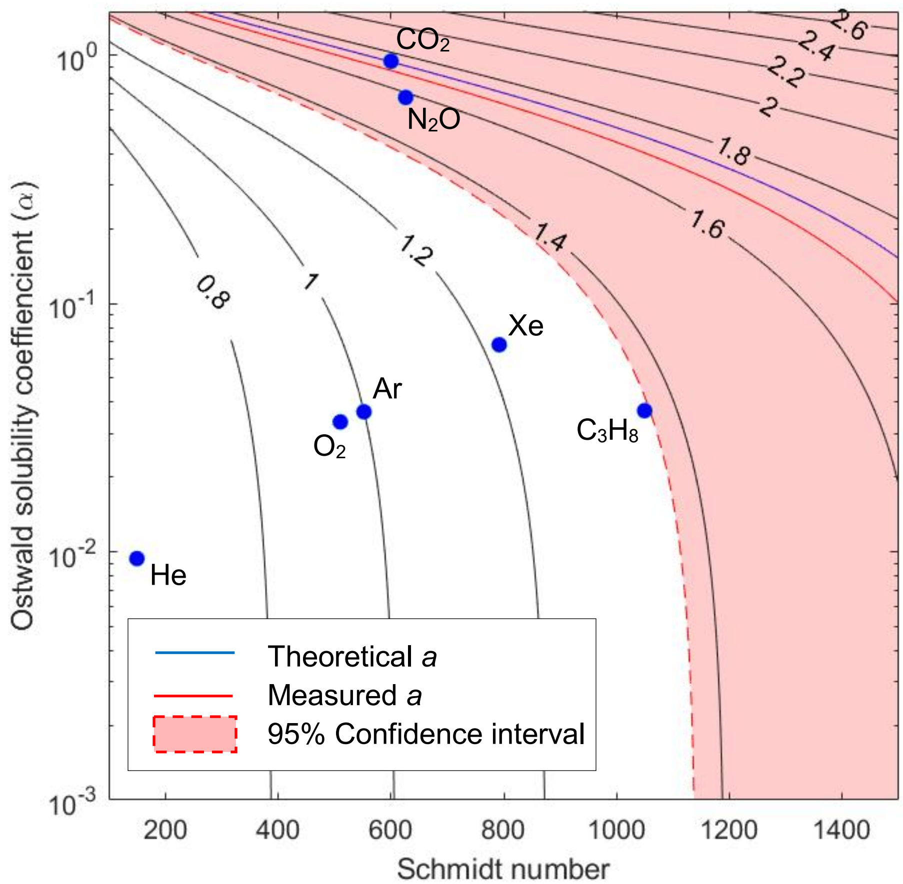

Figure 3. Contours are the ratio of the modeled bubble-mediated gas exchange rate (according to Woolf et al., 2007) of Ar to other gases ($K_{b,Ar}/K_{b,gas2}$) where $K_{b,gas2}$ is dependent on both solubility (represented by α, the Ostwald solubility coefficient) and Schmidt number. Ar falls on the contour equal to 1 as all values are referenced to Ar ($K_{b,Ar}/K_{b,gas2}$). The solid red line corresponds to the measured value for *a*, averaged across all the releases performed ($\bar{a}$). The blue line represents the theoretical value for *a* calculated according to Hall & Madinger 2018. At high solubilities, scaling between gases depends on both the Schmidt number effects and the solubility, while at low solubilities it is dependent on the Schmidt number only.

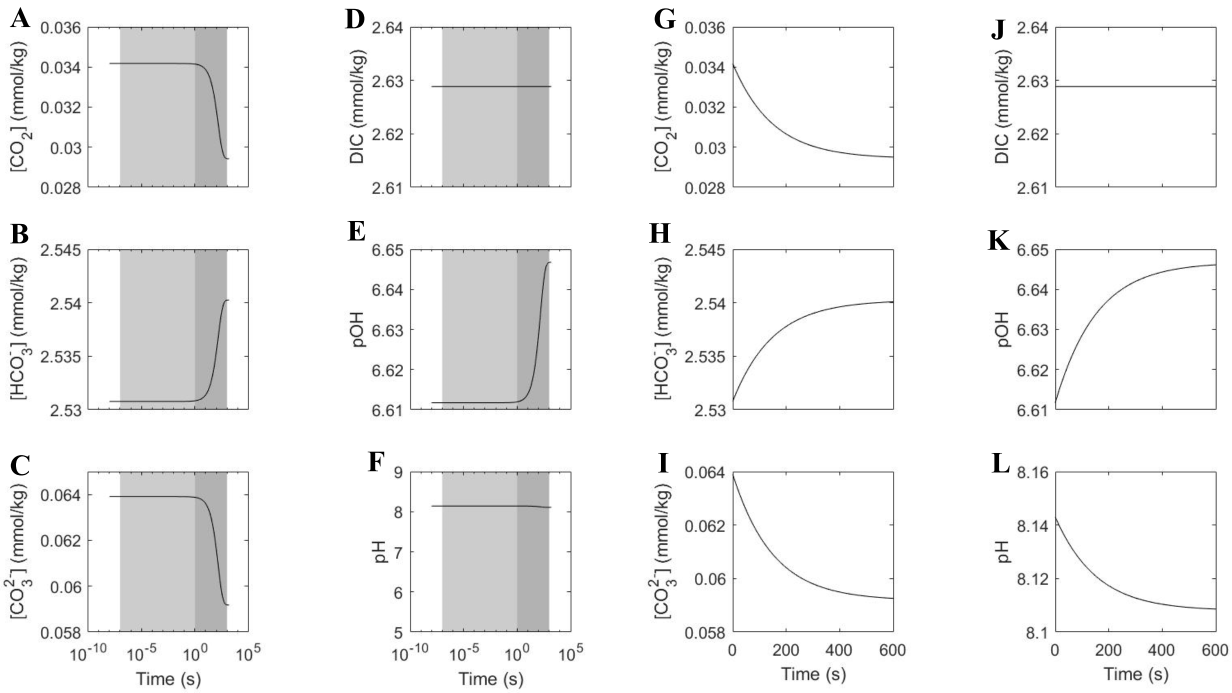

Figure 4. Example of an output of the reaction kinetics model (Stream: RIC, Date: 21 March 2019). Figures A-F depict changes in concentrations of [CO_2], [DIC], [HCO_3^-], [CO_3^{2-}], pOH and pH vs time (log-scaled) that occur at a logarithmic time scale (from 10^{-8} s to 600 s). Grey shaded areas show at what time scales we observe changes in concentrations (no change from 10^{-7} s to 10^0 s, but we observe changes in concentration from 10^0 to 10^3). Figures G-L show changes in concentration on a linear timescale (from 0 to 600 seconds) and are of the same order of magnitude as the timescales of gas exchange that occur in the stream. Measured values of [CO_2] and pH were used to estimate the initial conditions for the concentrations of [DIC], [HCO_3^-], [CO_3^{2-}] and pOH used in the kinetics model.

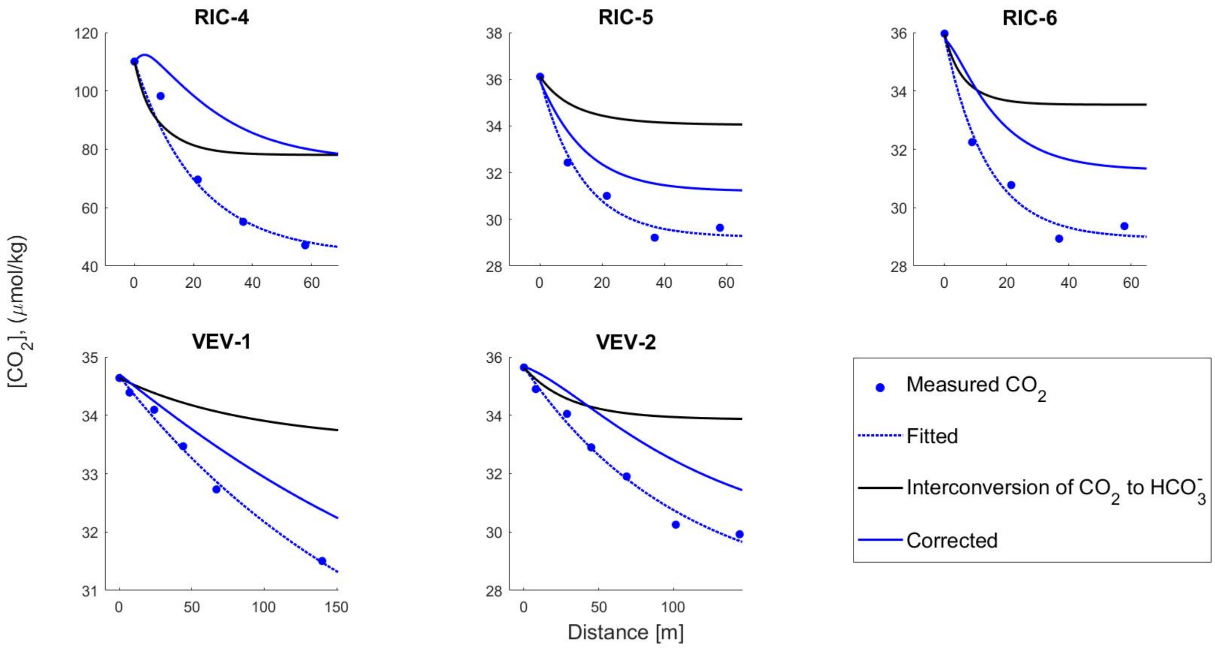

Figure 5. Modeled interconversion of CO_2 to HCO_3^-. The decrease in concentration of CO_2 that is due to chemical interconversion alone is shown in black. The corrected exponential decay of CO_2 in the stream is shown in blue and corresponds to $[CO_2]_{corrected} = [CO_2]_0 + [CO_2]_{measured} - [CO_2]_{interconversion}$. We observe that the effect of the chemical interconversion has the largest effect in the first few stations, as this is just after addition of the CO_2 gas to the stream. At stations farther from the addition site, the added CO_2 has theoretically had time to equilibrate, and therefore we observe changes in the concentration of CO_2 that are due to gas exchange with the atmosphere only. Therefore, the effect of interconversion is indirectly a function of stream flow rate (the faster the stream flow, the more stations will be affected).

Tables

Table 1. Study sites and stream characteristics including stream name, code, date of release, slope, reach length (*L*), average stream width (w), average stream depth (z) discharge (*Q*), mean stream velocity (v) and salt slug travel time (t).

Stream	Code	Date	Slope* [m m^{-1}]	L [m]	w [m]	z [m]	Q [m^3 s^{-1}]	v [m min^{-1}]	t [min]
Richard	RIC-1	29.Jan.18	0.14	65	1.9	0.11	0.030	8.6	8
Richard	RIC-2	16.Mar.18	0.14	65	1.4	0.11	0.011	4.2	16
Richard	RIC-3	30.May.18	0.14	57	4.8	0.98	1.023	13.0	4
Richard	RIC-4	21.Mar.19	0.14	69	1.7	0.13	0.016	4.1	17
Richard	RIC-5	15.Apr.19	0.14	65	2.4	0.08	0.017	5.3	11
Richard	RIC-6	30.Apr.19	0.14	65	2.5	0.44	0.050	2.7	5
Vièze	CHM-1	26.Jun.18	0.16	66	1.8	0.12	0.032	8.9	7
Vièze	CHM-2	04.Jul.18	0.16	67	2.5	0.08	0.021	6.4	11
Veveyse	VEV-1	12.Mar.19	0.10	151	6.7	0.17	0.591	30.5	5
Veveyse	VEV-2	28.Mar.19	0.10	146	6.1	0.34	0.411	12.0	6
Ferret	FET-1	08.Aug.18	0.06	142	3.1	0.12	0.143	23.7	6

**Slopes for all of the streams were measured using either digital GPS, a theolodite (Leica) and for one site (Veveyse) Google Earth by measuring the change in elevation from the top to the bottom of the reach and dividing by the length of the reach (m m^{-1}).*

Table 2. Descriptions of symbols used for the calculation of k_{CO_2} and k_{Ar} for each release

Symbol	Description (units) [constant]
k	Gas transfer velocity (m d^{-1})
k_{Ar}	Gas transfer velocity for Ar (m d^{-1})
k_{CO2}	Gas transfer velocity for CO_2 (m d^{-1})
a	Ratio of gas exchange rate of Ar to that of CO_2 [-]
A_x	Concentration ratio of Ar:N_2 (Corrected for background concentrations) [-]
A_0	Concentration ratio of Ar:N_2 at station 1 [-]
An_x	Concentration ratio of Ar:N_2 Normalized to A_0 [-]
C_x	Concentration of CO_2 (ppm)
C_0	Concentration of CO_2 at station 1 (ppm)
Cn_x	Normalized concentration of CO_2 [-]
An_0	Normalized concentration ratio of Ar:N2 at station 1 [-]
Cn_0	Normalized concentration of CO_2 at station 1 [-]
K_d	Gas exchange rate (m^{-1})
$K_{d,\,Ar}$	Gas exchange rate for Ar (m^{-1})
$K_{d,CO2}$	Gas exchange rate for CO_2 (m^{-1})
K_{Ar}	Gas exchange rate for Ar (d^{-1})
K_{CO2}	Gas exchange rate for CO_2 (d^{-1})
σ_A	Standard deviation of normally distributed residual errors for the statistical model of Ar [-]
σ_C	Standard deviation of normally distributed residual errors for the statistical model of CO_2 [-]
x	Distance along the reach (m)
a_j	Value of a in each stream j [-]
$\bar{a}$	Average value for a [-]
σ_a	Variation of a_j among streams, with a half-normal prior distribution
v	Nominal stream velocity (m s^{-1})
z	Average stream depth
k_{600}	Gas transfer velocity scaled to a common Schmidt number of 600 (m d^{-1})

Table 3. Measured gas exchange rates for Ar and CO_2 and calculated values. Scaling factors (a) are reported with 95% credible intervals.

Site	$K_{d,Ar}$ [m^{-1}]	K_{Ar} [d^{-1}]	k_{Ar} [m d^{-1}]	K_{d,CO_2} [m^{-1}]	K_{CO_2} [d^{-1}]	k_{CO_2} [m d^{-1}]	a [-]
RIC-1	0.046	566	65	0.044	543	62	1.15 (0.70,1.68)
RIC-2	0.056	336	36	0.028	169	18	1.93 (1.53,2.40)
RIC-3	0.035	650	640	0.016	308	302	1.99 (1.48,2.65)
RIC-4	0.049	289	39	0.027	159	21	1.79 (1.36,2.30)
RIC-5	0.057	436	34	0.028	214	17	1.80 (1.34,2.34)
RIC-6	0.057	224	99	0.028	109	48	1.96 (1.49,2.55)
CHM-1	0.043	559	66	0.026	332	39	1.70 (1.31,2.11)
CHM-2	0.043	392	32	0.028	256	21	1.55 (1.21,1.94)
VEV-1	0.011	496	86	0.006	260	45	1.84 (1.37,2.43)
VEV-2	0.008	145	49	0.010	176	59	1.12 (0.84,1.49)
FET-1	0.008	268	31	0.003	95	11	1.75 (1.27,2.36)

Table 4. Site chemistry data was recorded in the field for streams sampled March 2019 and onwards. These parameters were assessed at each station in the reach, however the averages for the entire reach are presented here for each release. The pH was measured on the free scale.

Code	Date	pH	Alkalinity (µmol/kg)	T (°C)	$[CO2]_0$ (µmol/kg)
RIC-4	21.Mar.19	7.90	1384.55	3.76	110.05
RIC-5	15.Apr.19	8.67	1346.40	4.06	36.11
RIC-6	30.Apr.19	8.55	1327.43	4.37	35.96
VEV-1	12.Mar.19	8.24	1658.31	2.01	34.64
VEV-2	28.Mar.19	8.26	1672.41	2.66	35.64